# Higher Order Mode Heating Analysis for the ILC Superconducting Linacs

Christopher Nantista
Karl L.F. Bane
Chris Adolphsen
SLAC

2010 Workshop on Higher-Order-Mode Damping in Superconducting RF Cavities (HOM10)
Cornell University, October 11-13, 2010

# Introduction

The superconducting cavities and interconnects in the 11 km long linacs of the International Linear Collider (ILC) are to operate at 2K, where cooling costs are very high.  It is thus important to minimize cryogenic heat loads, which, in addition to an unavoidable static load and the dynamic load of the fundamental 1.3 GHz accelerating rf, includes higher order mode (HOM) power deposited by the beam.

Modes trapped in the accelerating cavities are damped through the attached HOM coupler ports.  Modes above beampipe cutoff travel between beamline components and are damped by ceramic absorbers located between the 8 or 9-cavity cryomodules and thermally tied to the 70 K cryogenic envelope.

Because they extend well beyond a single cavity, brute force calculations of the higher frequency, non-trapped modes is limited by computing capacity. We present, instead, an approach that uses ccomponent scattering matrices at discrete frequencies to predict how such power will distribute itself along the beamline and study the effectiveness of the ceramic dampers in limiting the heat deposited in the 2K cryogenic system. The scattering matrices of beamline components are calculated for monopole modes propagating in the beampipe with the field solver HFSS.

# ILC Cavity Scattering Matrices

Ansoft HFSS was used to calculate *scattering matrices* for propagating monopole modes of beamline components with 39 mm radius beampipes at frequencies: 4, 8, 12, 16, and 20 GHz (1, 2, 3, 4, and 5 modes).

9 cell,
1.3 GHz
cavities:

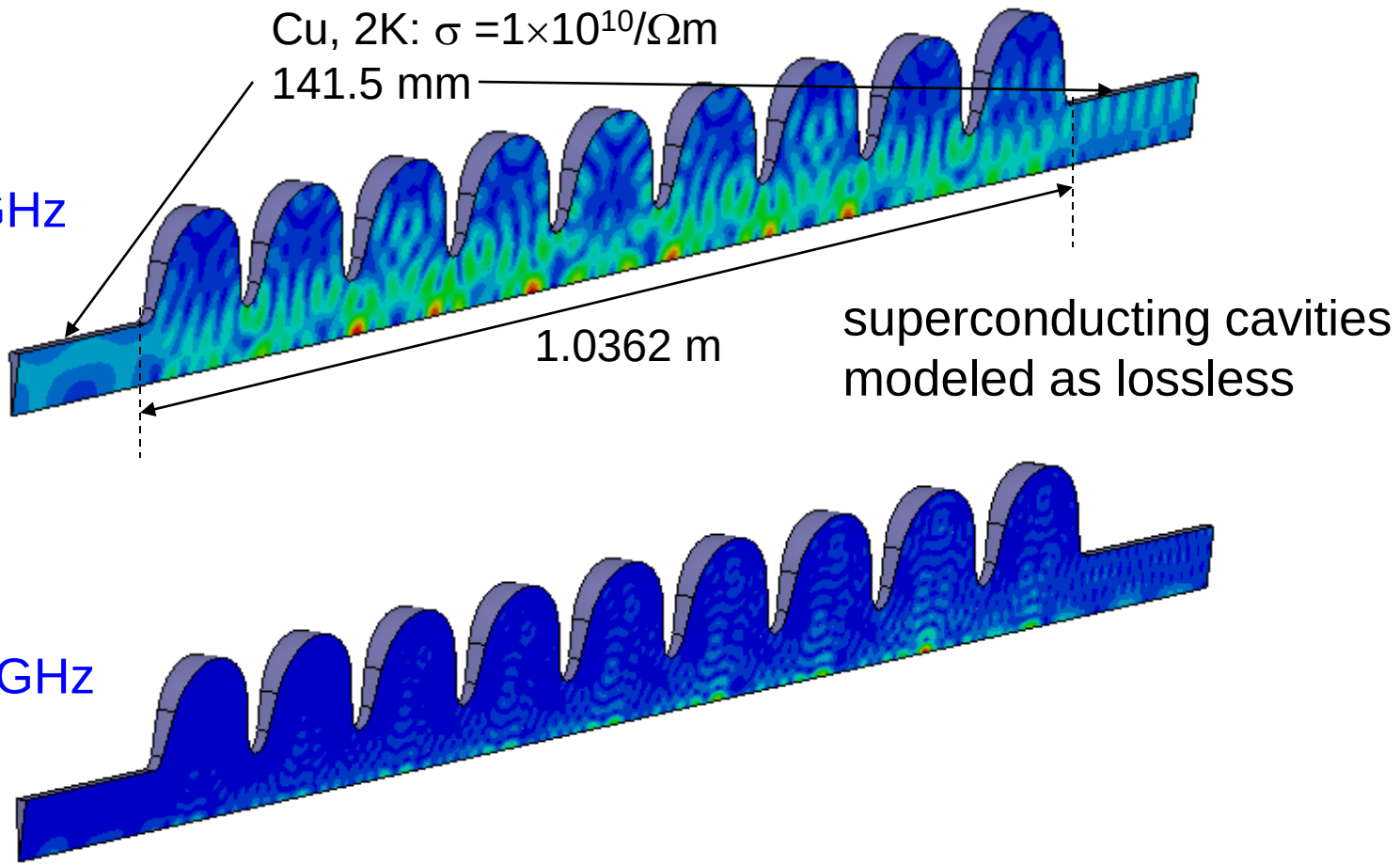

# Ceramic HOM Absorber

For lack of a better idea, we *approximate* $\tan\delta_l$ for 10 mm ring @ 70K as linearly dropping from 0.2 to 0.08 between 4 GHz and 20 GHz, based on the plots at right.

$\tan\delta_l$ = 0.2, @ 4 GHz
0.17, @ 8 GHz
0.14, @ 12 GHz
0.11, @ 16 GHz
0.08, @ 20 GHz

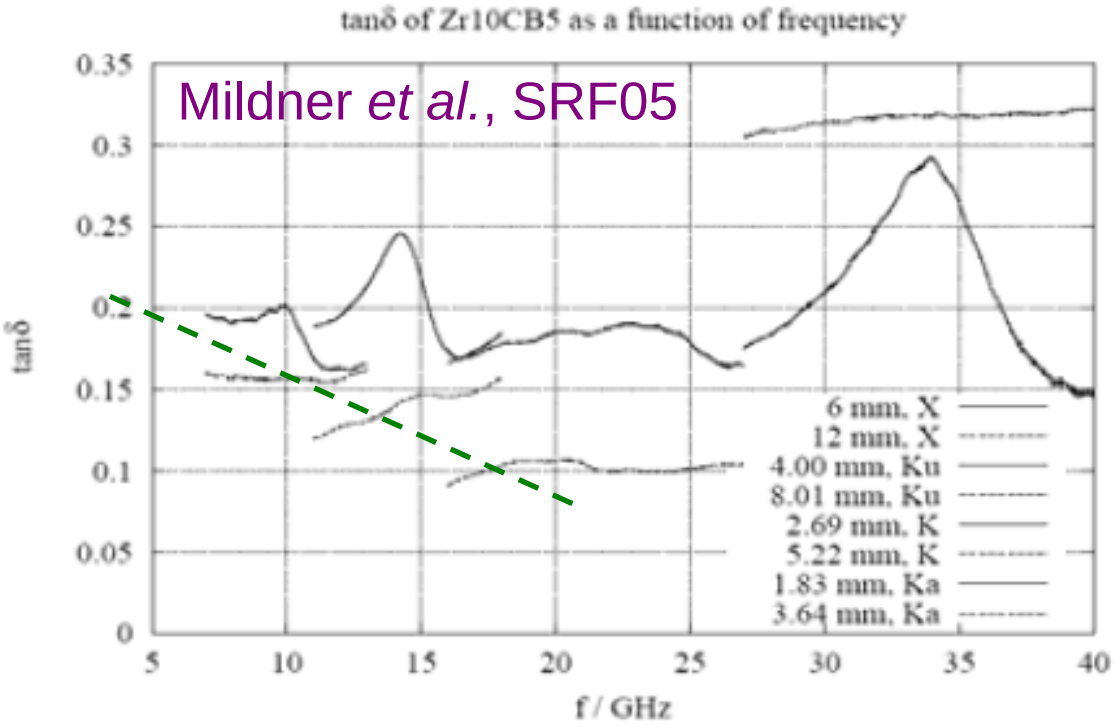


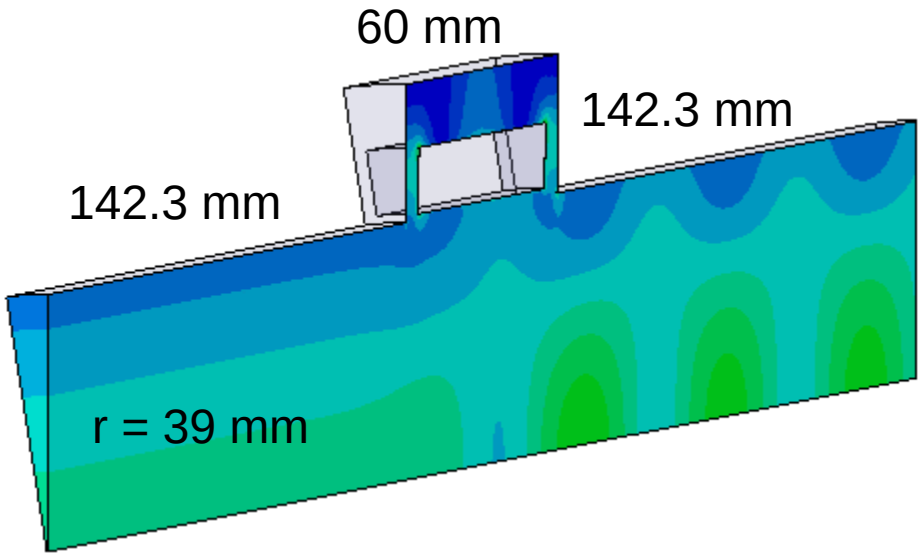


4 GHz: $\varepsilon = 15$, $\tan\delta_l = 0.2$

| Freq | | S:WavePort1:1 | S:WavePort2:1 | Gamma | Lambda |
|---|---|---|---|---|---|
| 4 (GHz) | WavePort1:1 | ( 0.27433, 51) | ( 0.91448, -44) | ( 56.778, 90) | 0.11066 |
| | WavePort2:1 | ( 0.91448, -44) | ( 0.27422, 50.9) | ( 56.778, 90) | 0.11066 |

8.85% absorbed

@ 8 GHz: 42% and 73% absorbed

@ 12 GHz: 30%, 54%, and 64% absorbed

# Bellows

~60 mm beampipe bellows with 10 convolutions were included between beamline elements.

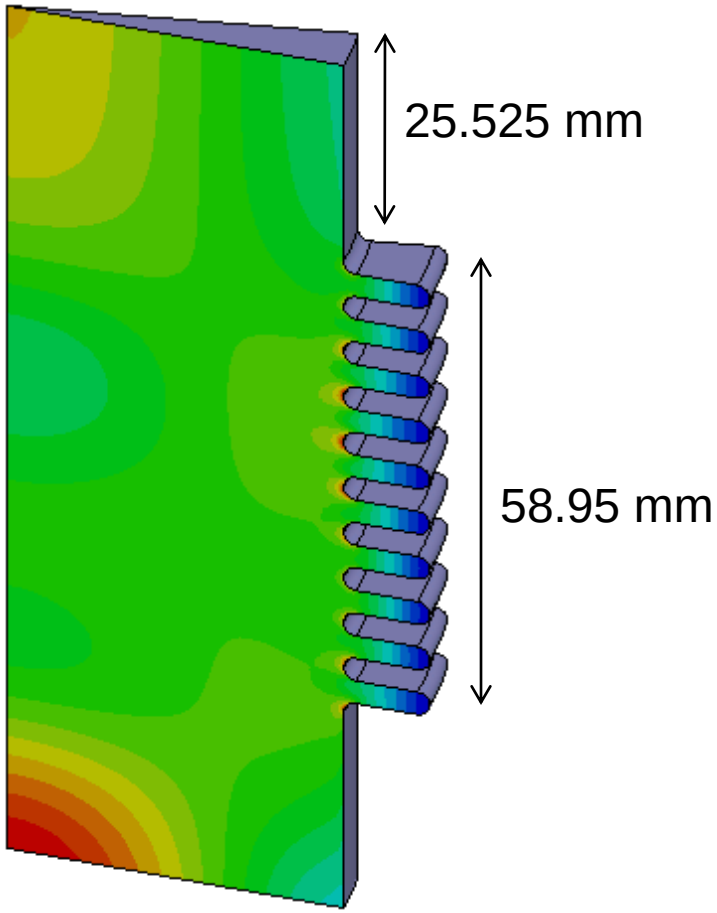


Finite conductivity: $\sigma = 1 \times 10^{10}/\Omega m$ only in convolutions (beampipe loss added analytically)

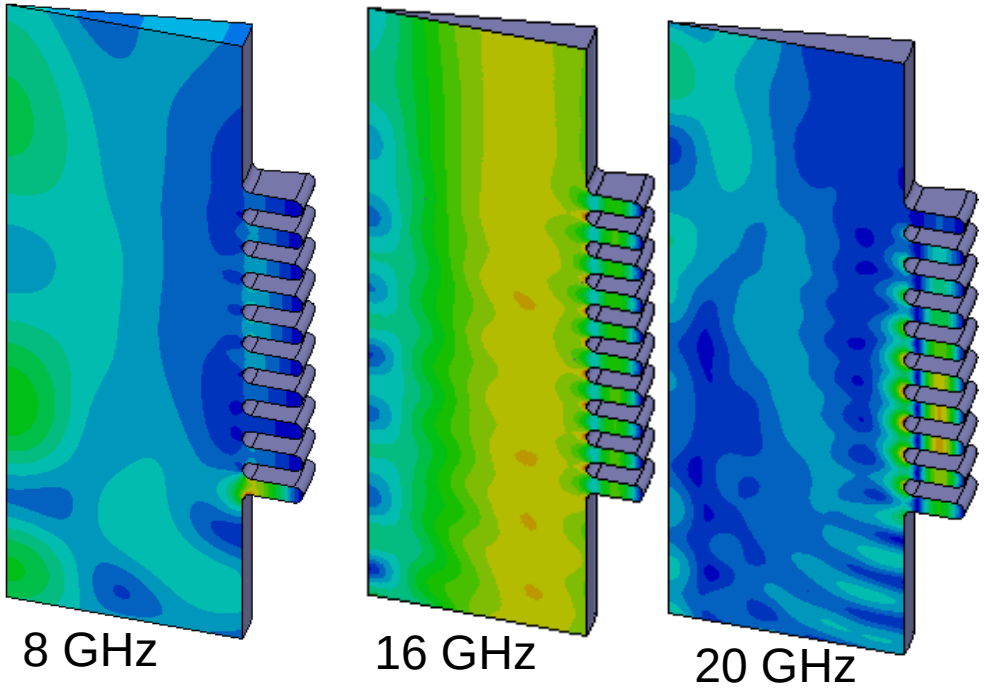

# Scattering Matrices for Beampipe Sections

$\sigma = 10^{10}\ \Omega^{-1}\mathrm{m}^{-1}$ (Cu @ 2K)

$\delta_s = (\mu_0 \pi f \sigma)^{-1/2}$

$R_s = 1/(\sigma\delta_s) = \sqrt{\mu_0 \pi f/\sigma}$

$a = .039$ m

$j_{0,1\text{-}5} = 2.4048, 5.5201, 8.6537, 11.7915, 14.9309$

Bessel roots for $TM_{01}$-$TM_{05}$

$$k_0 = 2\pi f / c, \quad k_{c,n} = j_{0,n}/a$$

$$\beta_n = \sqrt{k_0^{\,2} - k_{c,n}^{\,2}}, \quad \alpha_n = \frac{R_s}{aZ_0}\frac{k_0}{\beta_n}$$

$$\gamma_n = \alpha_n + i\beta_n$$

$$r_n(z_2) = r_n(z_1)e^{-\gamma_n(z_2-z_1)}$$

$$l_n(z_1) = l_n(z_2)e^{-\gamma_n(z_2-z_1)}$$

Scattering matrices of a beampipe section can be calculated analytically, as shown here. As for the bellows, copper plating at 2K was assumed for beampipes.

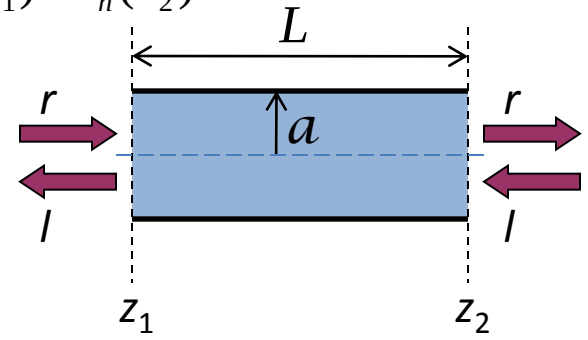


$$\mathbf{S}(f,L) = \begin{pmatrix} 0 & \begin{pmatrix} e^{-\gamma_1 L} & 0 & \cdots & 0 \\ 0 & e^{-\gamma_2 L} & \ddots & \vdots \\ \vdots & \ddots & \ddots & 0 \\ 0 & \cdots & 0 & e^{-\gamma_N L} \end{pmatrix} \\ \begin{pmatrix} e^{-\gamma_1 L} & 0 & \cdots & 0 \\ 0 & e^{-\gamma_2 L} & \ddots & \vdots \\ \vdots & \ddots & \ddots & 0 \\ 0 & \cdots & 0 & e^{-\gamma_N L} \end{pmatrix} & 0 \end{pmatrix},$$

$$\begin{pmatrix} l_1(z_1) \\ \vdots \\ l_N(z_1) \\ r_1(z_2) \\ \vdots \\ r_N(z_2) \end{pmatrix} = \mathbf{S} \begin{pmatrix} r_1(z_1) \\ \vdots \\ r_N(z_1) \\ l_1(z_2) \\ \vdots \\ l_N(z_2) \end{pmatrix}$$

# Beampipe Losses

In general, loss for beampipe lengths (losslessly) modeled as part of the other elements and loss and phase for any additional (or less) beampipe was combined into the elements of their scattering matrices as follows.

$$\mathbf{S}_{mn} \Rightarrow C_m \mathbf{S}_{mn} C_n$$

$$\text{where } C_m = \exp[-\alpha_m l_0 - (\alpha_m + i\beta_m)\Delta l\,]$$

with $l_0$ = modeled beampipe length,
$\Delta l$ = extra pipe length,
and the $\alpha$'s and $\beta$'s as defined on the last slide.

Except for:

- gap in cavity string (drift) where quadrupole magnet is located
- absorber beampipes, whose loss must be separated from that of the ceramic

# Cascading Multiple Objects

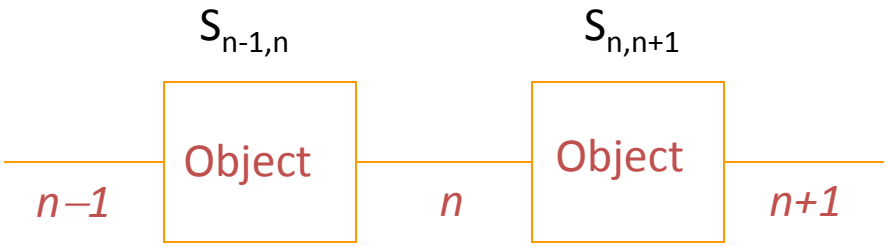


## To solve for the fields at all junctions:

- Create a matrix equation from the set of equations:

  $r_n = r_{n-1}(S_{12})_{n-1,n} + l_n(S_{22})_{n-1,n}$

  $l_n = r_n(S_{11})_{n,n+1} + l_{n+1}(S_{21})_{n,n+1}$

  with $n$ = 1,…$N$, where $N$ is number of objects.
- Impose boundary conditions.
- Include drive vector, *d.*
- Then solve $Ax = d$; matrix dimension is 2($N$+1).

With $M$ modes, matrix dim is $2(N+1)M$, (l&r × $N$+1 junctions × $M$ modes).

Total # of beamline objects in rf unit = 66. At 5 modes, order = 670.

# Period Boundary Conditions

The ILC linacs have a periodicity of a 3-cryomodule rf unit; two CM's have 9 cavities, and one has only 8 and one quadrupole magnet.

With an HOM absorber between each CM, our string of beamline objects is as indicated below (+bellows):

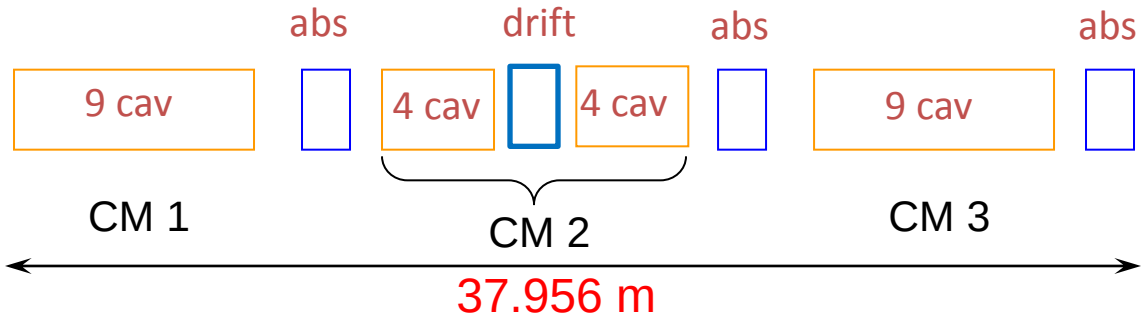


The steady state fields at the end of one period should be the same as those at the beginning, except for a phase determined by the total period length and the speed-of-light velocity of the driving beam.

So, we apply the folowing periodic boundary conditions:

$$r_{1,m} = r_{(n+1),m}\exp(-i\varphi_{tot}),$$
$$l_{(n+1),m} = l_{1,m}\exp(i\varphi_{tot}),$$
$$\varphi_{tot} \equiv \omega L_{tot}/c$$

# Driving Terms

As a driving term, we add to the right going wave in the lowest mode after each cavity unit amplitude with appropriate phase.

i.e. the elements of the driving vector *d* are:

$R_{i,1} = \exp(i\omega z_i/c)$, $R_{1,2-M} = 0$;  i = junction after a cavity

$R_{i,m} = 0$;  $i \neq$ junction after a cavity

$L_{i,m} = 0$;

with $z_i$ the distance along the beamline.

- Since we're interested in relative power into HOM absorber (70K) and 2K system, absolute amplitude is unnecessary.
- It would be more realistic to include drive power in all modes, left and right, for all objects, but knowledge of their relative amplitudes and phases would be needed to do so meaningfully (perhaps we can obtain these?)
- The power is scattered into the other modes anyway. We check the effect of driving different modes.

# Power Calculations

After solving the matrix equation for all the I's and r's, we calculate power dissipated in each object as the sum of incoming power minus the sum of outgoing power:

For object (n,n+1):

$$p_{n,n+1} = \sum_m \left( |r_{n,m}|^2 + |I_{n+1,m}|^2 - |I_{n,m}|^2 - |r_{n+1,m}|^2 \right) + |r_{n+1,1}|^2 - |r_{n+1,1} - d_{n+1,1}|^2,$$

The last two terms correct the outgoing power to the right in the first mode by subtracting the driven amplitude.

For a check, calculate power put into the system:

$$\rho_{err} = 1 - \sum_n \left( |r_{n,1}|^2 - |r_{n,1} - d_{n,1}|^2 \right) / p_{tot},$$

where $p_{tot}$, is the sum of all the object powers.

# Results

Wave Amplitudes at 4 GHz (1 mode)

blue - right (red - absorber)

brown - left

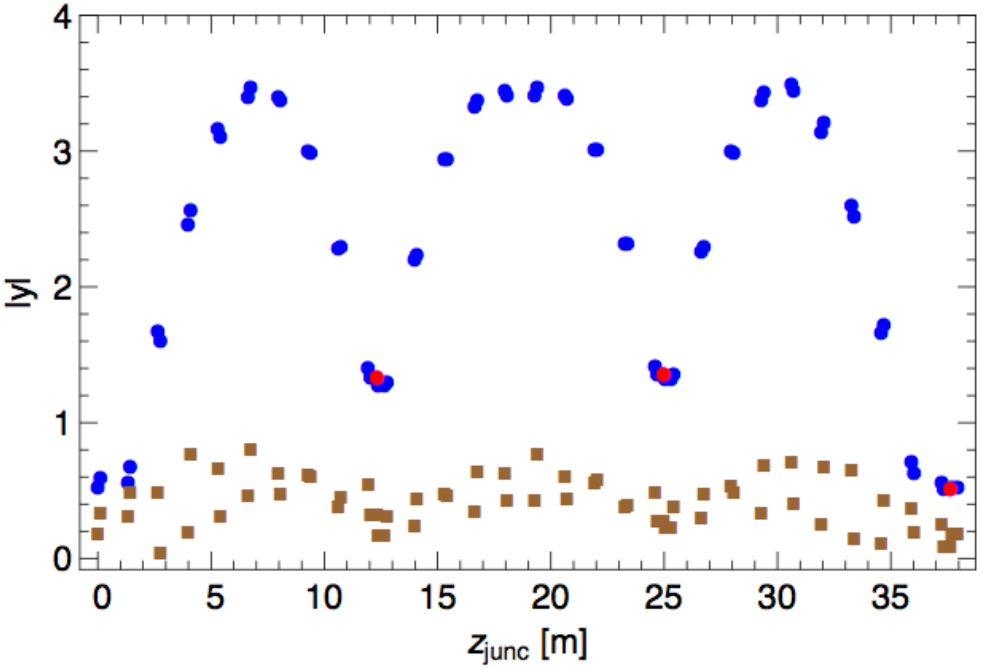


The relatively large (17.2%) power into 2K here is due to the absorbers being at relative nodes in the field pattern.

$p_{2K}/p_{tot}$ for Different Frequencies

(nominal and statistics*)

| f [GHz] | nom | ave | rms | 0.9 quant |
|---|---|---|---|---|
| 4 | 17.2 | 15.3 | 5.2 | 21.7 |
| 8 | 0.3 | 0.4 | 0.1 | 0.5 |
| 12 | 0.4 | 0.4 | 0.1 | 0.6 |
| 16 | 0.4 | 6.2 | 12.7 | 18.0 |
| 20 | 0.7 | 6.4 | 13.6 | 15.4 |

*As a sensitivity check, the cavity beampipe lengths were randomly varied (800 samples) with an rms $\sigma$ of 2 mm.

→ Relatively sensitive to spacing at 16 GHz and 20 GHz.

# Power Deposition Along the RF Unit at 4 GHz

(absorber losses shown in red)

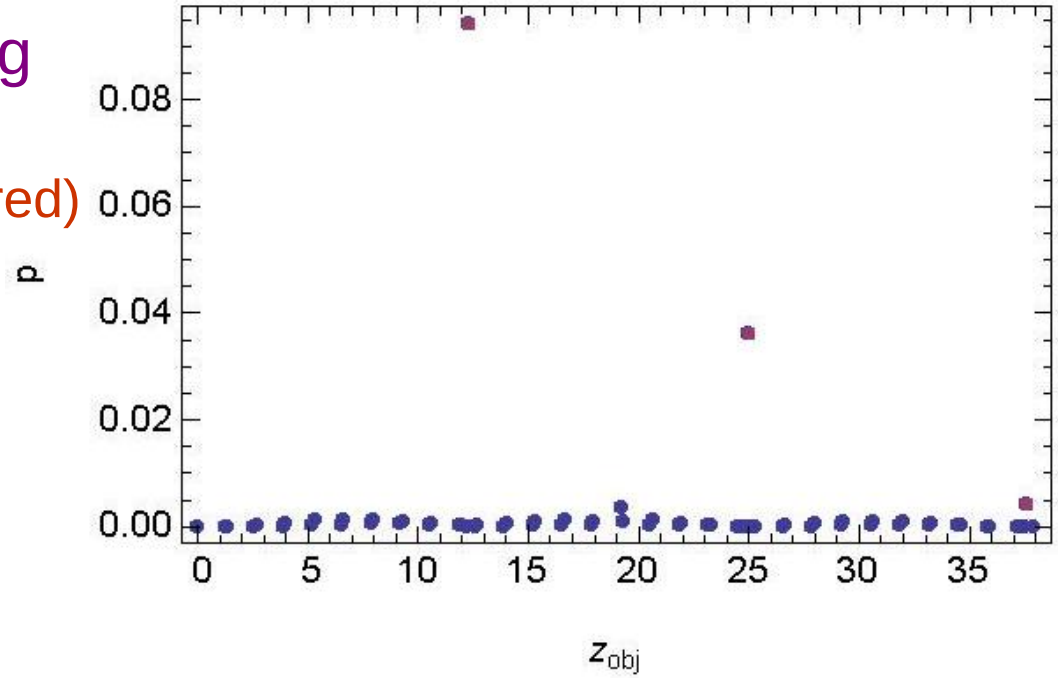


(Finer vertical scale)

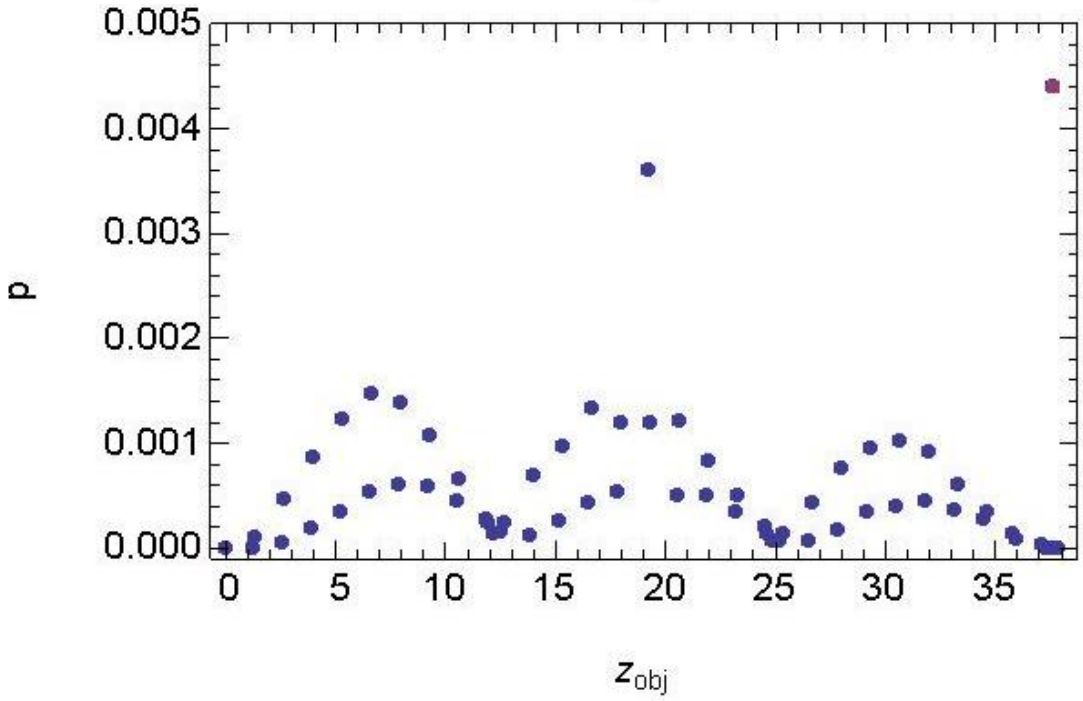

# Spacing Scan

One could repeat the calculations over many more frequencies to understand the power deposition in the gaps, although the approach will break down around mode cutoff frequencies, where evanescent fields cannot be ignored.

Instead, for our 5 sample frequencies, we systematically lengthened the cavity beam pipes, up to $\Delta z_{max}=2\pi/\beta_M$, and take the statistics of the results as indicators of absorber efficiency over the frequency intervals.

$p_{2K}/p_{tot}$ vs. Systematic Change of Cavity Length $\Delta z$ at 16 GHz (2000 steps)

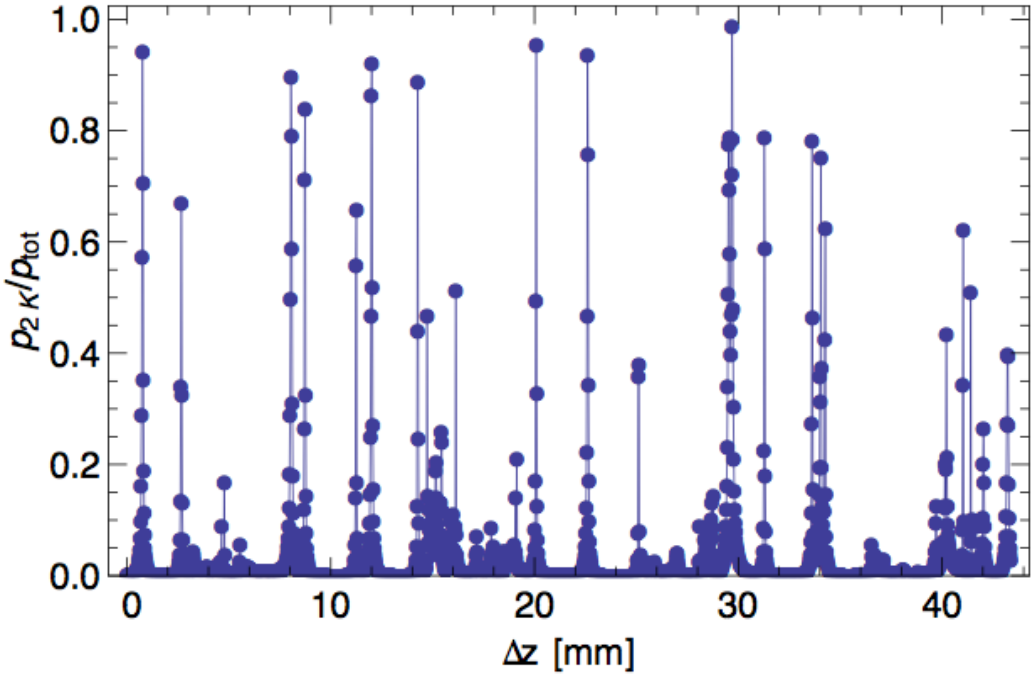


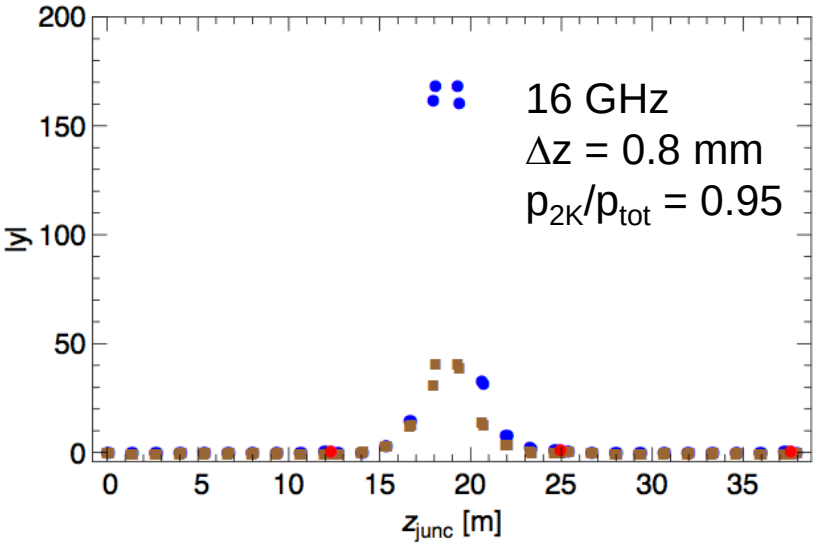


Some high values correspond to patterns w/ nodes at the absorbers, but many represent highly localized patterns such as the above.

# Statistics and Driving Mode Dependence

Table 2: Statistics for $p_{2K}/p_{tot}$ when varying cavity beam pipe length systematically ( in [%] ).

| f [GHz] | ave | rms | 0.9 quant |
|---|---|---|---|
| 4 | 8.0 | 7.0 | 15.7 |
| 8 | 2.8 | 6.6 | 5.9 |
| 12 | 1.4 | 3.8 | 2.2 |
| 16 | 4.0 | 11.8 | 7.0 |
| 20 | 5.9 | 10.5 | 13.5 |

Table 3: For $f = 16$ GHz, when the beam driving mode is $m$: Statistics for $p_{2K}/p_{tot}$ when varying cavity beam pipe length systematically ( in [%] ).

| m | average | rms | 0.9 quant |
|---|---|---|---|
| 1 | 4.0 | 11.8 | 7.0 |
| 2 | 3.2 | 9.1 | 5.2 |
| 3 | 4.1 | 11.1 | 8.1 |
| 4 | 3.4 | 9.4 | 6.5 |

Numbers don't seem to depend dramatically on which mode we drive, suggesting that results would be similar with all modes driven.

# Alternate Beamline Layout

Calculations were repeated with the objects rearranged. Specifically, an absorber was moved adjacent to the quadrupole “drift”, the longest section of lossy beampipe.

Comparing the folowing tables to those on previous slides reveals a noticeable improvement with this arrangement.

Table 1: Nominal result and statistics for $p_{2K}/p_{tot}$ when varying cavity beam pipe length randomly, with $\sigma_z = 2$ mm ( in [%] ).

| f [GHz] | nom | ave | rms | 0.9 quant |
|---|---|---|---|---|
| 4 | 6.9 | 6.4 | 1.3 | 8.1 |
| 8 | 0.1 | 0.5 | 0.1 | 0.6 |
| 12 | 0.2 | 0.5 | 0.1 | 0.7 |
| 16 | 0.1 | 4.2 | 11.2 | 8.8 |
| 20 | 0.1 | 5.8 | 13.2 | 14.3 |

Table 2: Statistics for $p_{2K}/p_{tot}$ when varying cavity beam pipe length systematically ( in [%] ).

| f [GHz] | ave | rms | 0.9 quant |
|---|---|---|---|
| 4 | 5.2 | 2.8 | 9.1 |
| 8 | 2.4 | 6.1 | 5.3 |
| 12 | 0.7 | 1.3 | 1.4 |
| 16 | 1.6 | 5.8 | 2.6 |
| 20 | 4.1 | 7.5 | 8.4 |

Table 3: For $f = 16$ GHz, when the beam driving mode is $m$: Statistics for $p_{2K}/p_{tot}$ when varying cavity beam pipe length systematically ( in [%] ).

| m | average | rms | 0.9 quant |
|---|---|---|---|
| 1 | 1.6 | 5.8 | 2.6 |
| 2 | 1.7 | 5.5 | 2.6 |
| 3 | 2.0 | 6.5 | 3.3 |
| 4 | 1.6 | 4.6 | 2.9 |

# Conclusions

• To study the effectiveness of the ceramic dampers in absorbing the HOM power generated by the beam, we have presented an S-matrix based formulation of power flow in a string of three ILC cryomodules,

• From detailed calculations at 5 sample frequencies, we have obtained estimates of the damper effectiveness in the frequency range up to 20 GHz

• We find that the expectation value in this range of the fraction of HOM power that is *not* absorbed by the dampers is 1.5%–8.0%

• According to our calculations, a highly localized field pattern can occur that avoids the absorbers and renders them ineffective.

• Note that in this simplified, cylindrically-symmetric model, the effect of the fundamental power and HOM couplers is not included.